7-2023

Optic Nerve Head Gene Transcription Sequelae to a Single Elevated IOP Exposure Provides Insights Into Known Responses to Chronically Elevated IOP

Diana C. Lozano
Oregon Health and Science University

Hari Jayaram
NIHR Moorfields Biomedical Research Centre

William O. Cepurna
Oregon Health & Science University

Shandiz Tehrani
Oregon Health & Science University

Lina Gao
Oregon Health & Science University

Citation Details

Authors

Diana C. Lozano, Hari Jayaram, William O. Cepurna, Shandiz Tehrani, Lina Gao, Suzanne S. Fei, Dongseok Choi, Elaine C. Johnson, and John C. Morrison

Optic Nerve Head Gene Transcription Sequelae to a Single Elevated IOP Exposure Provides Insights Into Known Responses to Chronically Elevated IOP

Diana C. Lozano,[1,2] Hari Jayaram,[3] William O. Cepurna,[1] Shandiz Tehrani,[1] Lina Gao,[4,5] Suzanne S. Fei,[4,5] Dongseok Choi,[1,6] Elaine C. Johnson,[1] and John C. Morrison[1]

[1]Department of Ophthalmology, Casey Eye Institute, Oregon Health & Science University, Portland, Oregon, United States
[2]Department of Chemical Physiology, Oregon Health & Science University, Portland, Oregon, United States
[3]NIHR Moorfields Biomedical Research Centre, London, United Kingdom
[4]Bioinformatics & Biostatistics Core, Oregon National Primate Research Center, Oregon Health & Science University, Portland, Oregon, United States
[5]Biostatistics Shared Resources, Knight Cancer Institute, Oregon Health & Science University, Portland, Oregon, United States
[6]School of Public Health, Portland State University, Portland, Oregon, United States

Correspondence: Diana C. Lozano, 515 SW Campus Dr., Portland, OR 97239-4197, USA; lozano@ohsu.edu.

PURPOSE. To clarify the optic nerve head (ONH) gene expression responses associated with a single, axon-damaging exposure to elevated IOP in relation to the composite cellular events previously identified in models of chronically elevated IOP.

METHODS. Anesthetized rats were exposed unilaterally to an 8-hour pulse-train controlled elevation of IOP (PT-CEI) at 60 mm Hg, while others received normotensive CEI at 20 mm Hg. ONH RNA was harvested at 0 hours and 1, 2, 3, 7, and 10 days after either CEI and from naïve animals. RNA sequencing was performed to analyze ONH gene expression. DAVID Bioinformatics tools were used to identify significant functional annotation clusters. Gene function was compared between PT-CEI and two models of chronic ocular hypertension from the literature.

RESULTS. The number of significantly changed genes peaked immediately ($n = 1354$) after PT-CEI (0 hours). This was followed by a lull (<4 genes per time point) at 1 and 2 days after PT-CEI. Gene activity increased again at 3 days (136 genes) and persisted at 7 (78 genes) and 10 (339 genes) days. Significant gene functional categories included an immediate upregulation of *Defense Response* at 0 hours, followed by upregulation in *Cell Cycle*, a reduction in *Axonal*-related genes at 3 to 10 days, and upregulation of *Immune Response*–related genes at 10 days following PT-CEI. The most commonly upregulated gene expression across our PT-CEI study and two chronic models of ocular hypertension were cell cycle related.

CONCLUSIONS. The PT-CEI model places in sequence ONH gene expression responses previously reported in models with chronically elevated IOP and may provide insights into their role in optic nerve damage.

Keywords: glaucoma, optic nerve head, RNA-seq, immune response, cellular proliferation, axons, intraocular pressure

Lowering IOP, a mainstay of current glaucoma therapy, can reduce vision loss in all forms of glaucoma.[1–3] Unfortunately, some patients still lose vision despite seemingly "successful" pressure control. In other patients, medical, laser, and surgical approaches may be ineffective, poorly tolerated, or too risky. New treatments are still needed to reduce axonal injury and retinal ganglion cell loss in patients with glaucoma. This requires better understanding of the cellular mechanisms of pressure-induced optic nerve damage.

Several animal models of chronic IOP elevation have been used to study cellular responses in the optic nerve head (ONH). As this is the site of initial injury, such approaches are likely to reveal mechanisms of axonal injury in glaucoma.[4–6] Gene array and deep sequencing studies have revealed a large number of downregulated and upregulated mRNA expression in these models.[7–11] These include alterations in several cellular pathways, including those regulating cellular division, cytokine response, cell signaling pathways such as Jak2/Stat3, and immune responses. This has led to more targeted investigations, such as cellular immune response and increased interest in the role of neuroinflammation in these models and in glaucoma.[12–14] Coupled with immunohistochemical analyses to identify affected cell types within the ONH, these studies have dramatically added to the list of cellular events that may accompany axonal injury

due to elevated IOP and may lead to future targets for intervention and neuroprotection.

This knowledge, even if observed in mild and early glaucoma, does not confirm their role in the glaucomatous process or, specifically, their relationship to axonal injury. In chronic models, where pressure elevation is ongoing, some axons are actively undergoing injury while other axons are already injured.[15–19] Thus, gene expression changes detected in chronic models reflect genes that are actively contributing to the injurious process as well as those that are responding to the injury. Others may be protective. Also, IOP-related gene changes likely reflect responses by several cell types. Unraveling the relative importance of all of these events in chronic models is therefore complicated by the simultaneous presence of a wide range of cellular events and time frames.

One approach to this problem is to experimentally limit IOP exposure to a discrete event. To this end, the Controlled Elevation of IOP (CEI) glaucoma model was developed in Brown Norway rats.[20] Anesthetized animals are exposed for a discrete period of time, typically several hours, to increased IOP in a cannulated eye via an attached elevated reservoir containing balanced salt solution. In our initial report, using a limited quantitative real-time reverse transcription PCR screen, we found that a single CEI exposure produced patterns of optic nerve (ON) injury and ONH gene expression similar to those previously observed in our original, hypertonic saline chronic IOP elevation model.[21] In addition, we found evidence that these gene expression changes occurred sequentially, continuing many days after the pressure insult had ceased. From these observations, we hypothesized that a single pressure elevation event results in a cascade of gene expression responses, both acute and delayed, that represent most changes seen in chronic models. This might provide an opportunity to understand sequential gene responses and their relationship to pressure and role in axonal injury. However, a comprehensive analysis is still needed.

In this study, we performed an RNA sequencing (RNA-seq) analysis of ONH immediately after (0 hour) and 1, 2, 3, 7, and 10 days following a CEI exposure and compared these results with eyes exposed to normotensitve CEI (IOP = 20 mm Hg) and to results from ONH from anesthetized, uncannulated, naïve rats. We also compared gene expression responses over the entire recovery time period to similar published data sets from models of chronic glaucoma.[9,11] The results confirm that findings in tissues from chronic glaucoma models include events occurring in association with IOP elevation and likely axonal injury, as well as those occurring at variable times after injury. The importance of these results to the glaucomatous process is then considered on the basis of their temporal relationship to the IOP exposure and axonal injury.

METHODS

Rodent Model of Ocular Hypertension (Controlled Elevation of IOP)

Experiments were approved by the Oregon Health & Science University Institutional Animal Care and Use Committee and performed in accordance with the ARVO Statement for the Use of Animals in Ophthalmic and Vision Research.[22] Retired Brown Norway rats (∼8 months old) were kept in a standard 12-hour light/dark cycle with free access to food and water.

A single eye per animal was included in this study. Rats (four at a time) were anesthetized with isoflurane (2%) with 100% O_2 and active evacuation of expired gas. Animals were heated with circulating warm water pads and hydrated with hourly subcutaneous saline. Topical artificial tears or 0.5% proparacaine hydrochloride (Akorn, Lake Forest, IL, USA) were alternately applied every 15 minutes to both eyes. A clear-corneal track was created with a 31-gauge needle and the anterior chamber cannulated with a 1-in. polyurethane tubing (0.010 in. OD/0.005 in. ID; Instech Laboratories, Plymouth Meeting, PA, USA; part BTPU-010) connected to a larger diameter tygon tubing (Component Supply Company, Fort Meade, FL, USA; part TND80-040). This led, via a larger tube, to a pressure transducer and suspended reservoir containing sterile balanced salt solution-plus (Alcon Laboratories, Fort Worth, TX, USA, NDC 0065-0800-94, parts 1 and 2) for adjusting IOP.

Two paradigms were studied: a unilateral "pulse-train" controlled elevation of intraocular pressure (PT-CEI) of 60 mm Hg and a normotensive CEI of 20 mm Hg. The PT-CEI is a modified version of our original CEI model where IOP is returned to 20 mm Hg for 5 minutes every hour over the duration of the experiment—with a cumulative exposure to elevated IOP (60 mm Hg) of 8 hours (total experimental time was 8 hours and 40 minutes).[20] The purpose of this was (1) to maximize gene expression by increasing the ONH stress and strain response to changing pressure[23] and (2) to reduce the potential of an ischemic event by regularly returning IOP to normal levels. Thus, the PT-CEI was designed to identify the impact of elevated IOP on ONH gene expression. In the second paradigm, the normotensive CEI, IOP was kept at 20 mm Hg for 8 hours to provide a control for the effects of anesthesia and anterior chamber eye cannulation. In both paradigms, a single averaged IOP reading was checked by TonoLab rebound tonometry (Colonial Medical Supply, Franconia, NH, USA, USA) every 30 minutes to detect unanticipated low IOPs that might indicate leakage or cannula failure. At the end, IOP was reduced to 20 mm Hg for 5 minutes, the cannula removed, and the needle track allowed to self-seal. In a separate group of animals ($n = 4$; Supplementary Fig. S2), awake IOP was measured 1 week prior to PT-CEI and every day for the next 10 days. Baseline mean IOPs in the right eye (20 ± 2 mm Hg) and left eye (22 ± 1 mm Hg) were not significantly different ($P = 0.32$) and did not significantly change after PT-CEI ($P = 0.66$). Linear regression lines of mean IOP over days were not significantly different ($P = 0.54$) between PT-CEI–treated eyes and control eyes. These results indicate that IOP returns to baseline levels following PT-CEI. Thus, the gene expression findings reported here are most likely entirely the result of the PT-CEI exposure. Physiologic parameters (O_2 saturation, heart rate, temperature, and blood pressure), monitored by a Mouse Ox Plus Oximeter (STARR Life Sciences Corporation, Oakmont, PA, USA) and a CODA Noninvasive Blood Pressure System (Kent Scientific Corporation, Torrington, CT, USA), remained stable while animals were anesthetized throughout the entire experiment.[20,24]

Animals were euthanized at the end of IOP exposure (0 hours) or 1, 2, 3, 7, and 10 days after PT-CEI and/or normotensive CEI (60 animals, 60 ONH; $n = 6$ per PT-CEI time point and $n = 4$ per normotensive time point). Both paradigms were compared to eight naïve ONHs (one eye each from eight different animals) that were anesthetized prior to euthanasia and that had no eye cannulation. Animals were randomly preassigned to a specific experimental paradigm type (PT-CEI or normotensive CEI) and

time of euthanasia. Euthanasia was performed by decapitation under deep anesthesia and at approximately the same time of day (e.g., ~5 PM each day) for all animal groups.

ONH Dissection and RNA Extraction

Following euthanasia, enucleated globes were rapidly chilled in cold phosphate-buffered saline (PBS) and the anterior segment, lens, and retina removed. The posterior segment was laid flat on chilled wax and the ONH trephined out with a 1.5-mm biopsy punch (Acuderm, Ft. Lauderdale, FL, USA). After removing the remaining sclera and nerve sheath, the ONH was positioned in a custom-designed mold to allow separation of the anterior 0.4-mm ONH (Supplementary Fig. S1). Dissected ONHs were frozen in dry ice and stored immediately at –80°C until all samples were collected and ready for RNA extraction.

Prior to RNA extraction, all ONHs were randomized into RNA extraction groups (about eight ONHs per group) to limit possible batch effects. RNA was extracted with the MiRNEasy kit (Qiagen, Venlo, Netherlands) in accordance with the manufacturer's guidelines and as previously described.[25] The OHSU Gene Profiling Shared Resource unit analyzed total isolated RNA quality (RNA integrity number or RIN score) and measured concentration with the Agilent Bioanalyzer Pico Chip, Santa Clara, CA, USA. RIN scores and RNA concentrations (mean of 61–64 ng) were similar among naïve, PT-CEI, and normotensive CEI ONH.

RNA Library Preparation and Sequencing

Short read sequencing assays were performed by the Oregon Health & Science University Massively Parallel Sequencing Shared Resource. Briefly, samples were randomized into sequencing groups to further limit possible batch effect. Total RNA was used as a template for library preparation using the Ovation RNA-Seq System (NuGen, Redwood City, CA, USA). First-strand cDNA was generated from mRNA using NuGen's DNA/RNA chimeric primer mix, which is designed to avoid priming from ribosomal RNA. Then, cDNA underwent single primer isothermal amplification (SPIA) to generate a double-stranded cDNA. The cDNA was used to make a library with the TruSeq DNA-seq kit (Illumina, San Diego, CA, USA). Libraries were quantified using real-time PCR (Kapa Biosystems, Wilmington, MA, USA), mixed, and diluted as needed to reach appropriate cluster densities. Samples were then run on a HiSeq 2500 in RapidRun mode. Eight libraries were sequenced per lane. Each lane generated about 155 million clusters, which were sequenced using a single-read 100-cycle protocol. Fastq files were generated using base call files (.bcl) using the CASAVA package (Illumina). Fastq files are available online through the National Library of Medicine, National Center for Biotechnology Information–Sequence Read Archive under BioProject PRJNA942989.

RNA-Seq Data Analysis

The Oregon Health & Science University's Oregon National Primate Research Center Bioinformatics & Biostatistics Core performed quality RNA-seq assessment, alignment, and differential expression analyses. The quality of the raw sequencing files was evaluated using FastQC (https://www.bioinformatics.babraham.ac.uk/projects/fastqc/), and all samples had adequate quality. Trimmomatic was used to remove any remaining Illumina adapters.[26] Reads were

aligned to the Rnor_6.0 reference genome in Ensembl along with its corresponding annotation (release 85). STAR (v020201) was used to align the reads to the genome.[27] Since STAR utilizes the gene annotation file, it calculated the number of reads aligned to each gene. The function "RNA-SeQC" was utilized to ensure all alignments were of sufficient quality.[28]

Gene-level raw counts were filtered to remove genes with extremely low counts in many samples following published guidelines.[29] A total of 16,257 genes were retained for differential expression analysis. Counts were normalized using the trimmed mean of M-values method (TMM) and transformed to log-counts per million with associated observational precision weights using the voom method.[30,31] Genewise linear models accommodating factorial design between PT-CEI treatments and time points and adjusting for technical factors (library preparation batch, sequencing batch, and lane) were employed for differential expression analyses using limma with empirical Bayes moderation and false discovery rate (FDR) adjustment to identify differentially expressed genes in prespecified contrasts.[32,33] Significantly regulated genes can be found in Supplementary Tables S1 and S2.

Gene Functional Interpretation

Genes with expression ≥130% or ≤77% relative to naïve values and with a 10% FDR were considered significant. Significantly upregulated and downregulated genes were independently uploaded to the DAVID Bioinformatics website. Functional Annotation Clustering analyses were performed to identify significant Gene Ontology clusters.[34,35] Significant clusters were defined as those having an enrichment score ≥1.3. Representative Gene Ontology terms for each cluster and their associated P value were saved for each time point. Then, GOPlot functions in R Statistical Language were used to visualize these long lists of Gene Ontology terms.[36] This function plots bubbles for each Gene Ontology term, where the size of the bubble is proportional to the number of genes within that term. The z score is plotted on the x-axis and P value (log) on the y-axis. For this specific plot, the z score represents the number of significantly upregulated genes minus downregulated genes, all divided by the total number of significantly regulated genes per Gene Ontology term. In general, the z score hints if a cluster is more likely to be downregulated (negative value) or upregulated (positive value).

Optic Nerve Grading

Myelinated optic nerves were collected, postfixed in equal parts of buffered 5% glutaraldehyde and 4% paraformaldehyde, embedded in Spurr's resin, cross-sectioned, and stained with toluidine blue for light microscopic evaluation.[37] Each nerve was graded for injury, on a scale from 1 (normal nerve) to 5 (extensive degeneration affecting nearly all axons), by at least five independent masked observers, and the mean defined the injury grade for that nerve.[7]

Gene Functional Comparison Between PT-CEI and Models of Chronic Ocular Hypertension

Significantly regulated genes following PT-CEI (will be referred to as the PT-CEI/Seq study) were compared with our previous microarray analysis performed in ONHs with

small, focal optic nerve lesions following 5 weeks of chronically elevated IOP (will be referred to as the Chronic/Array study).[9] In both the PT-CEI/Seq and Chronic/Array studies, the same ONH region (the first 400 µm posterior to Bruch's membrane opening) was analyzed. In the Chronic/Array study, there were 877 significantly regulated genes with expression greater than 130% or less than 77% and with *P* < 0.05. Since the microarray was sequenced to the mouse genome, we uploaded the PT-CEI/Seq study Ensembl rat gene IDs to the Ensembl–Biomart website to identify orthology/homologous mouse genes.[38] We next identified genes that were significant in the Chronic/Array study and in the PT-CEI/Seq study. Significant genes from the PT-CEI/Seq had expression >130% or <77%. The FDR criterion was loosened, from 10% to 20%, because these were exploratory analyses to identify commonalities between studies. DAVID functional annotation clustering analyses were performed on genes that were significant by expression, and statistical significance and results were visualized with GOPlots.

We also compared our PT-CEI/Seq findings with those of a feline congenital glaucoma model (will be referred to as the FCG/Seq study). This is a spontaneously occurring, recessively inherited form of feline congenital glaucoma in which cats develop elevated IOP at 10 weeks of age.[11] Animals in this study were young, and the identified cellular responses represent early changes prior to significant irreversible axon loss. Out of the 384 significantly regulated cat genes from the FCG/Seq study, we found 283 rat orthologous/homologous genes in the PT-CEI/Seq study. DAVID functional annotation clustering analyses were also performed on these genes, and results were visualized with GOPlots.

Immunolabeling and Quantifying ONH Glia in Normal Rats

Globes from a separate group of animals were collected and processed for immunohistochemistry. A control group (*n* = 20 globes from 20 different animals) and PT-CEI–exposed globes were collected at the same time points as in the RNA-seq study (e.g., 0 hours and 1, 2, 3, 7, and 10 days; *n* = 7–8 animals per experimental time point). Animals were perfused transcardially under anesthesia with buffered 4% paraformaldehyde, as previously described.[39] Briefly, globes were embedded in paraffin and longitudinally sectioned vertically. On the first day, sections were deparaffinized, rehydrated in PBS, blocked with SEA BLOCK blocking buffer (Thermo Fisher Scientific, Waltham, MA, USA), and incubated overnight in 4°C with primary antibodies or IgG controls. Primary antibodies tested included goat anti-Sox2 for astrocyte nuclei (0.3 µg/mL; Santa Cruz Biotechnology, Dallas, TX, USA, sc-17320), mouse anti-Olig2 for oligodendroglia (1 µg/mL; Millipore Sigma, St. Louis, MO, USA, MABN50), and goal anti-Iba1 for microglia and macrophages (0.6 µg/mL; Novus Biologicals, Centennial, CO, USA, NB100-1028). The following day, slides were incubated for 30 minutes in 0.2% secondary antibody (Alexa Fluor 594 anti-mouse IgG or Alexa Fluor 594 anti-goat; Life Technologies, Grand Island, NY, USA), and slides were coverslipped after applying a drop of antifade mounting media (Prolong Gold; Life Technologies) containing DAPI.

Slides were photographed (20× magnification) with a fluorescence microscope (Olympus America, Center Valley, PA, USA). ONH nuclei were semiautomatically identified using a MATLAB program (MATLAB R2015a and Image Processing Toolbox; The MathWorks, Natick, MA, USA). We focused our nuclear counts on the first 400 µm posterior to Bruch's membrane opening, comparable to the amount of ONH analyzed in the current RNA-seq study.

RESULTS

Elevated IOP Confirmation and Resulting Nerve Injury

First, we investigated IOP measurements in the PT-CEI and normotensive CEI animals. The mean ± SD TonoLab rebound tonometer measurements were 56 ± 2 mm Hg when IOP was elevated in the PT-CEI model and 18 ± 3 mm Hg when IOP was lowered to normal-awake IOP. The mean TonoLab reading during normotensive CEI was 19 ± 2 mm Hg. Focal and mild optic nerve axonal injury was visible by light microscopy at 7 days (mean grade = 1.72 ± 0.55; *P* = 0.0002) and at 10 days (mean grade = 1.95 ± 1.03; *P* = 0.004) following PT-CEI relative to controls. There was no significant visible injury in the normotensive CEI nerves at these same time points (mean grade = 1.03 ± 0.04; *P* = 0.88) relative to controls. These results agree with our previously published work in the original CEI model indicating that significant and mild optic nerve injury appears at 7 days after pressure exposure and persists at least by 14 days.[20]

PT-CEI ONH Responses Are Due to Elevated IOP and Not Anesthesia or Cannulation

The maximum number of significantly regulated genes occurred immediately at the end of the PT-CEI model (0 hours, 1354 genes), followed by a lack of significant IOP-responsive genes at 1 day (0 genes) and 2 days (4 genes: *LOC100359539*, *Lcn2*, *Cenpe*, *Creb3l1*). Gene activity increased again at 3 days (132 genes) and persisted at 7 (78 genes) and 10 (339 genes) days (Fig. 1). These genes were found to cluster into multiple significant Gene Ontology terms, to be presented below. All significantly regulated genes following PT-CEI are included in Supplementary Table S1. Normotensive CEI yielded 18 significant genes only at 0 hours (Supplementary Table S2). These normotensive-CEI genes did not cluster into any significant Gene Ontology term, and none were significant in the PT-CEI paradigm. These results indicate that ONH mRNA expression following PT-CEI is due to elevated IOP and not a by-product of anesthesia or anterior chamber cannulation.

Additionally, we searched for hypoxia-related expression changes immediately following PT-CEI (0 hours). We found that *Hif1a* was significantly elevated (142%), while its negative regulator *Hif3a* was also significantly increased (252%). Other hypoxia-related genes were not detected (*Epo*, *Hif2a*), significantly reduced (*Arnt2*), or unchanged (*Hif1an*, *Arnt*). Additionally, *Hyou1* (hypoxia up-regulated 1, 109%), previously identified to be selectively expressed in astrocytes under hypoxic conditions, remained unchanged following PT-CEI.[40] These findings indicate that optic nerve injury from PT-CEI is likely not due to ischemia. This is consistent with optical coherence tomography angiography studies in anesthetized animals showing that retinal blood flow is not compromised at these same levels of IOP.[24,41,42]
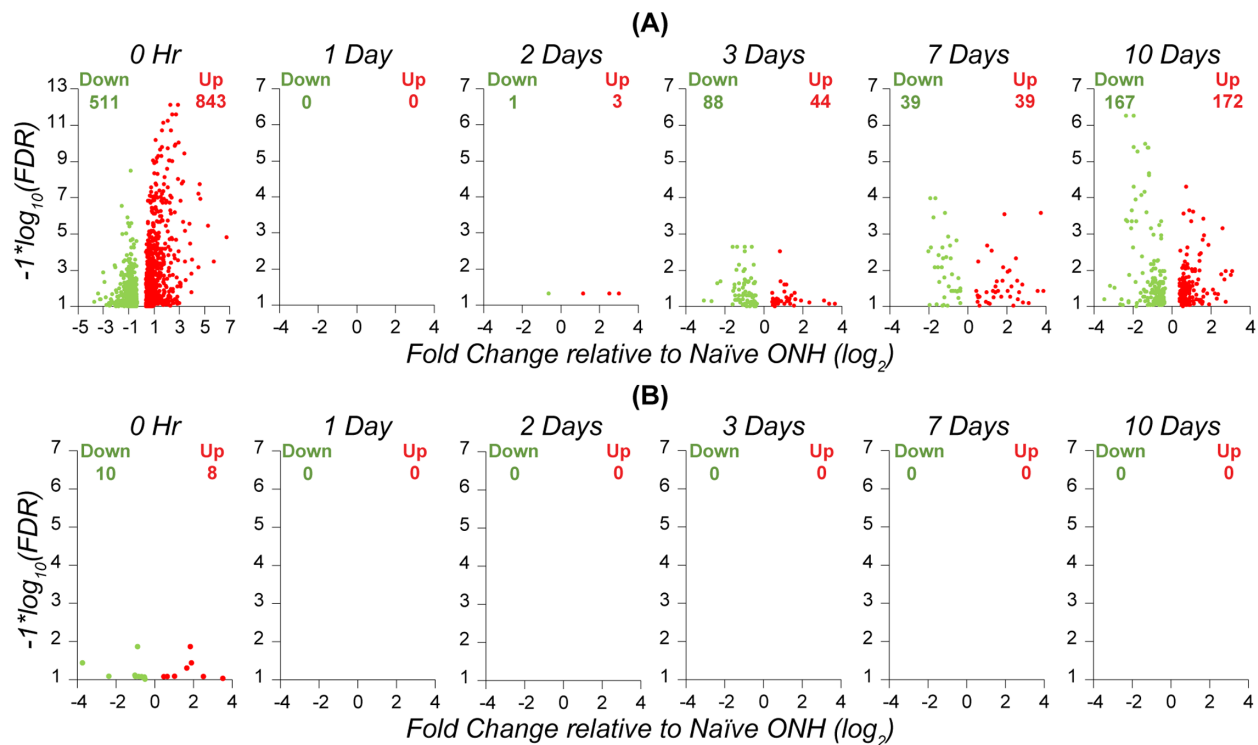
FIGURE 1. The biphasic ONH gene expression responses following PT-CEI are due to elevated IOP exposure, not anesthesia or cannulation of the eye. (**A**) Volcano plots of significantly regulated genes following a single 8-hour PT-CEI relative to naïve ONH. The highest number of significantly regulated genes was seen at the end of the PT-CEI (0 hours), followed by a lull at 1 day and 2 days. Gene activity increased again at 3 days and persisted at 7 and 10 days. (**B**) Volcano plots of significantly regulated genes following normotensive CEI relative to naïve ONH. Only 18 genes were significantly changed immediately at the end of the normotensive CEI (0 hours), and no genes were significant at other time points. Significantly downregulated genes are shown in *solid green*, and significantly upregulated genes are shown in *solid red*.

Persistently Regulated Genes at Several Time Points Following PT-CEI

Five genes were significantly regulated at several time points following PT-CEI (*Lcn2*, *Timp1*, *Runx1*, *Wee1*, and *Nefm*). Following PT-CEI, lipocalin 2 (*Lcn2*) was upregulated at all studied time points, except on day 1, and the mean fold change across all of these time points was 549% ± 108%, relative to naïve ONH. *Lcn2* belongs to the *Defense Response* Gene Ontology cluster at 0 hours and the *Immune Response* Gene Ontology cluster at 10 days. Tissue inhibitor matrix metalloproteinase 1 (*Timp1*) was upregulated at 0 hours and 3, 7, and 10 days following PT-CEI, and the mean fold change across these time points was 434% ± 198%, relative to naïve ONH. Runt-related transcription factor 1 (*Runx1*) was upregulated at 0 hours and 3, 7, and 10 days, and the mean fold change of these time points was 275% ± 127% relative to naïve ONH. *Wee1* (WEE1 G2 checkpoint kinase) was significantly upregulated at 0 hours and 3, 7, and 10 days following PT-CEI. The mean fold change of *Wee1* across these time points was 136% ± 8% relative to naïve ONH. *Wee1* is part of the *Cell Cycle* Gene Ontology cluster. Lastly, the neurofilament medium chain (*Nefm*) was first significantly upregulated at 0 hours (153%), then significantly downregulated 3 days (38%), 7 days (31%), and 10 days (25%) following PT-CEI. *Nefm* is part of the *Axon/Synapse/Neuron Part* Gene Ontology clusters.

Interestingly, these five genes help establish the framework for the most represented gene functional categories following PT-CEI, which will be discussed below. These include (1) the upregulation of *Defense Response* immediately after PT-CEI (0 hours), (2) an upregulation in *Cell Proliferation*, (3) a steady and persistent downregulation in *Axonal-* and *Synapse*-related mRNA expression, and (4) a late-appearing *Immune Response* at 10 days.

Identification of Regulated Functional Gene Categories Following PT-CEI

The number of functional annotation clusters identified by DAVID analysis was highest at 0 hours (166 up- and 53 downregulated). Following the lull at 1 and 2 days, the number of clusters gradually increased to 22 at 3 days (5 up- and 17 downregulated), 25 at 7 days (9 up- and 16 downregulated), and 72 at 10 days (41 up- and 31 downregulated; Fig. 2). Importantly, the few significantly regulated genes at 2 days after PT-CEI and the few significant genes following normotensive CEI did not cluster. Significant clusters identified at 0 hours and 3, 7, and 10 days following PT-CEI will be presented below (Figs. 3–6).

Significant Gene Ontology Clusters Identified at 0 Hours and 3, 7, and 10 Days Following PT-CEI

Upregulation of ONH Defense Response Following PT-CEI at 0 Hours. There were 1354 regulated ONH genes immediately following PT-CEI (0 hours). For these, the top-rated, upregulated gene category was *Defense Response* (GO:0006952; Fig. 3A). This Gene
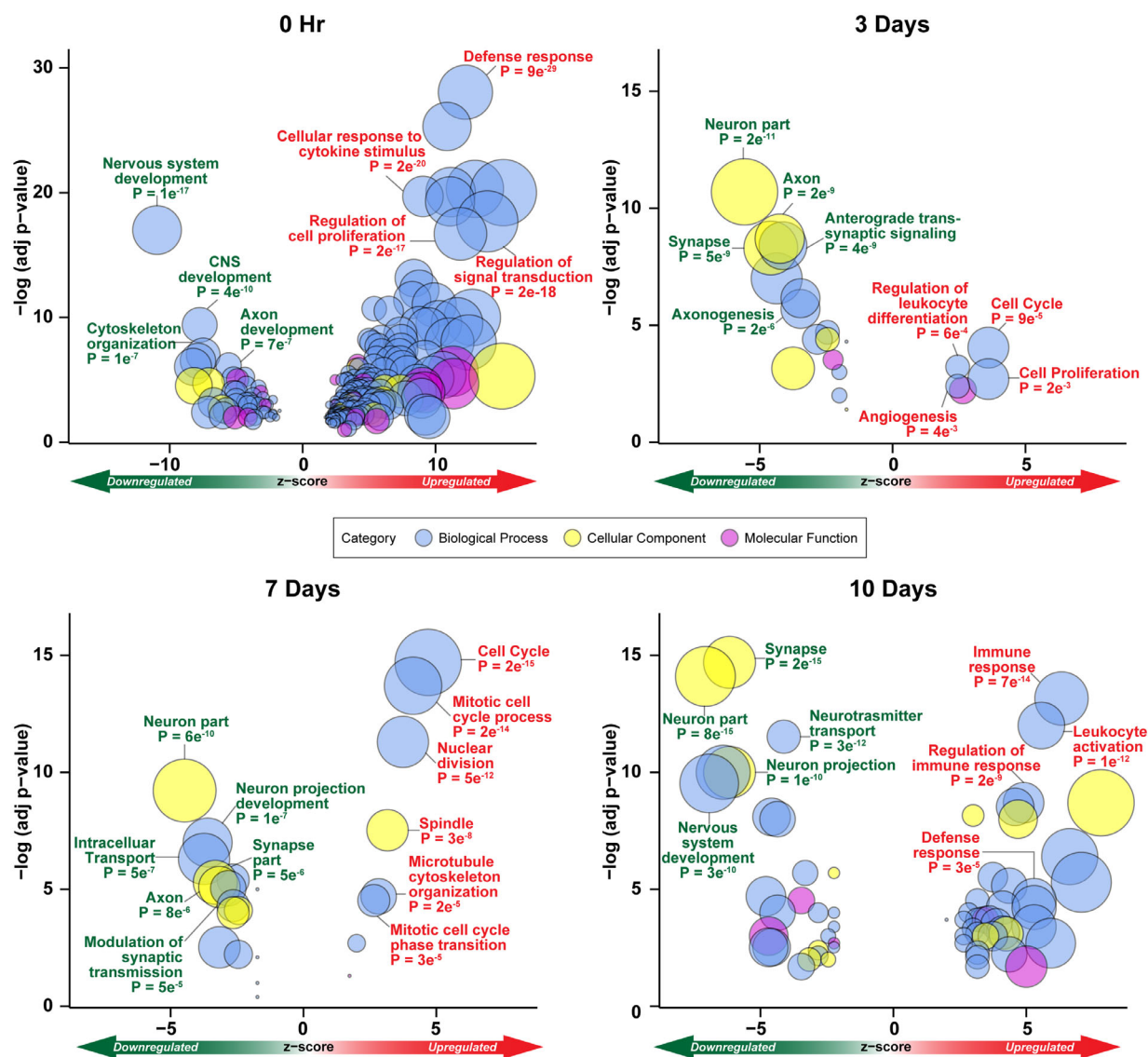
FIGURE 2. Functional assessment following PT-CEI. GOPlots of significantly regulated Gene Ontology (GO) clusters derived from DAVID analyses (clusters with EASE score ≥1.3). The *z* score hints if a GO cluster is more likely to be downregulated (negative value) or upregulated (positive value). Bubble sizes are scaled independently between plots and represent the number of genes within each term cluster. Specific GO terms of interest are highlighted, as well as their associated *P* value and number of genes in that term (shown in parentheses). Following PT-CEI, the most regulated time point was 0 hours, and this was followed by an absence of gene regulation for 1 and 2 days and an uptick in regulation for 3 to 10 days.

Ontology term is likely involved with the reaction generated in response to elevated IOP. Out of 150 genes in this category, *Il6* (5160%) and other Il6-type cytokines, for instance, *Il11* (1538%), *Lif* (1069%), and *Clcf1* (387%), were among the most upregulated (Fig. 3B). These Il-6 type cytokines initiate signaling via the Jak-Stat pathway. Therefore, we looked more closely at genes involved with the Jak-Stat pathway and found 27 significantly upregulated genes immediately following PT-CEI (Fig. 3B). These findings indicate that these genes are among the earliest ONH responses to elevated IOP. This *Defense Response* cluster becomes nonsignificant for the majority of the other time points following PT-CEI. However, an *Immune Response* cluster becomes significant at 10 days. Importantly, only 5 (*C1s*, *Ifnlr1*, *Jak3*, *Lcn2*, and *Tlr7*) out of the 150 *Defense Response*–related genes were found in the late-appearing *Immune Response* cluster, highlighting that

these two clusters are distinct from each other. Genes associated with the *Immune Response* cluster that appears later are discussed below.

Upregulation of Cell Proliferation Genes Following PT-CEI. *Cell Proliferation*–related Gene Ontology clusters were significantly upregulated at various time points following PT-CEI. There was one cluster at 0 hours, two clusters at 3 days, seven clusters at 7 days, and three clusters at 10 days. We first investigated the 0 hours genes, and gene expression was highest for *Fosl2* (987%) and *Junb* (425%; Fig. 4A). Both belong to the family of activating protein 1 (AP1) transcription factors that control cell proliferation, survival, and death.[43] Other AP1 genes that were significantly upregulated at 0 hours included *Fos* (297%) and *Fosl1* (987%). Lastly, Figure 4B highlights an additional 30 proliferation-related genes that were upregulated 3 to
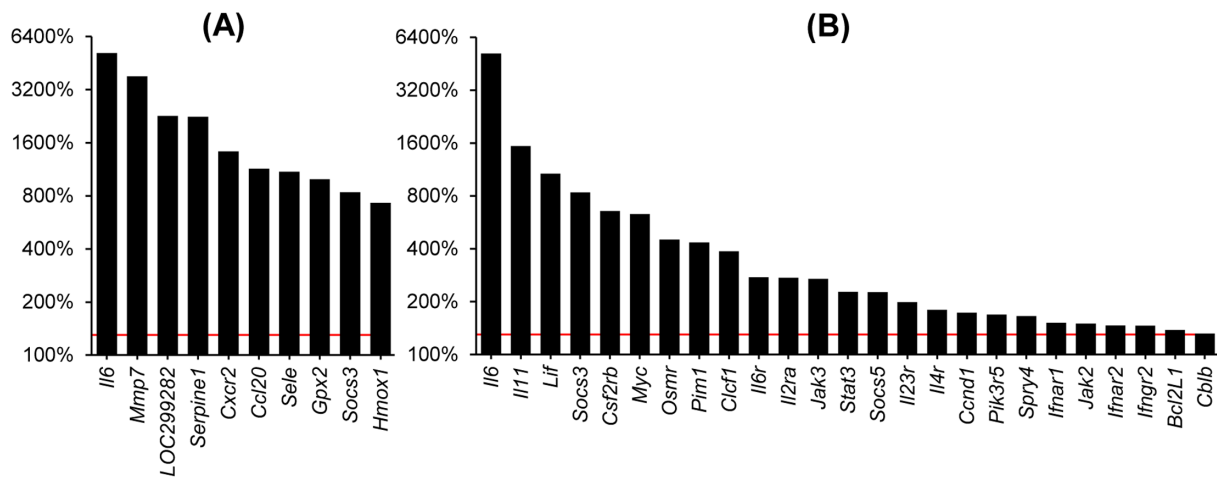
FIGURE 3. Upregulation of *Defense Response*–type genes immediately following PT-CEI. (**A**) The top 10 upregulated genes in the *Defense Response* Gene Ontology term immediately following PT-CEI (0 hours). (**B**) Il-6 type cytokines and Jak-Stat pathway genes were significantly upregulated immediately (0 hours) following PT-CEI. Note that the y-axis is in a $\log_2$ scale.

10 days following PT-CEI. Put together, genes in Figure 4A likely reflect signaling or regulation of ONH cell proliferation, while genes in Figure 4B are likely evidence of ONH cell proliferation.

Axonal-Related mRNA Expression Is Disproportionally Depressed Relative to Axonal Injury. We next evaluated *Axonal*-related Gene Ontology clusters identified from our DAVID functional analysis and found 21 unique genes within these clusters. Initially, these genes tended to be nonsignificantly upregulated at 0 hours, although *Nefm* upregulation (153%) was significant. This may reflect obstructed axonal transport during pressure elevation. At 3 days, expression of these genes reached a nadir, averaging about 50% of control values that was sustained through 10 days (Fig. 5). Interestingly, the depression in axonal mRNA expression was disproportionally greater than the extent of optic nerve injury, which was minimal, with grades less than 2 (equivalent to approximately <15% degenerating axons).

Delayed and Unique Immune Signals at 10 Days Following PT-CEI. The *Immune Response* (GO:0006955) Gene Ontology cluster was significantly upregulated at 10 days following PT-CEI. There were 40 *Immune Response*–related genes. Ten of these were identified as being involved in the Antigen Processing and Presentation Kyoto Encyclopedia of Genes and Genomes pathway (Fig. 6A). An additional set of genes was identified as being microglia/macrophage related and/or playing a role in their activation (Fig. 6B). The common microglia/macrophage marker, *Aif1*, became significantly upregulated at 10 days, while other microglia or macrophage markers (*P2ry12*, *Tmem119*, *Cx3cr1*) remained unchanged throughout the entire 10 days (Fig. 6C). We also noted that expression of genes in the delayed *Immune Response* category was not as dramatic as the *Defense Response* at 0 hours or the cellular proliferation and axonal gene expression responses described above.

Mild Extracellular Matrix Remodeling Develops After PT-CEI. Genes that indicate glial scar formation (*Gfap*, *Col4a1*, *Col6a2*, *Col5a2*) remained unchanged out to 10 days following PT-CEI. Only *Col4a5* (136%) and *Col12a1* (182%) were significantly upregulated at 10 days.

Several integrins, important mediators of cell extracellular matrix (ECM) adhesion, were significantly regulated at 0 hours (*Itga4*: 57%, *Itga5:* 305%, and *Itgad*: 164%) and 10 days (*Itgb1*: 136% and *Itgb2*: 169%). The ECM metalloproteinase inhibitor *Timp1* was the only ECM gene that was significantly upregulated at 0 hours (727%), 3 days (297%), 7 days (347%), and 10 days (363%). These results might indicate that the axonal injury that develops following PT-CEI is very mild with minimal early glial scar formation or that a more chronic pressure insult is required to produce significant glial remodeling. Lack of some changes, such as those for Glial fibrillary Acidic Protein (GfAP) mRNA, may indicate that while mRNA expression levels remain unchanged, significant protein reorganization may still occur.[44]

A Single, Short-Term Elevated IOP Exposure Can Model the Sequence of Events Seen in Chronic Ocular Hypertensive Models

We previously conducted a microarray study to determine gene expression changes in ONHs exposed to chronically elevated IOP (Chronic/Array study).[9] In that study, there was a group with small, focal optic nerve lesions (grades less than 2), comparable to that seen here following PT-CEI. Forty-four percent of genes that were significantly regulated in the Chronic/Array study were also significant at one or more of the time points in the current PT-CEI/Seq study. An additional 20% of significant Chronic/Array genes were significant by expression level but not by FDR in the PT-CEI/Seq study, while the remaining 36% of significant Chronic/Array genes were not significant in the PT-CEI/Seq study.

Focusing on the 44% of significant Chronic/Array genes that were also significantly changed in the PT-CEI study, we found 198 genes in common at 0 hours, 79 genes at 3 days, 29 genes at 7 days, and 99 genes at 10 days following PT-CEI. More than 90% of these genes were regulated in the same direction in both studies (Fig. 7A). Interestingly, 23 of the 150 significantly upregulated *Defense Response* genes at 0 hours in the PT-CEI/Seq study were also significantly
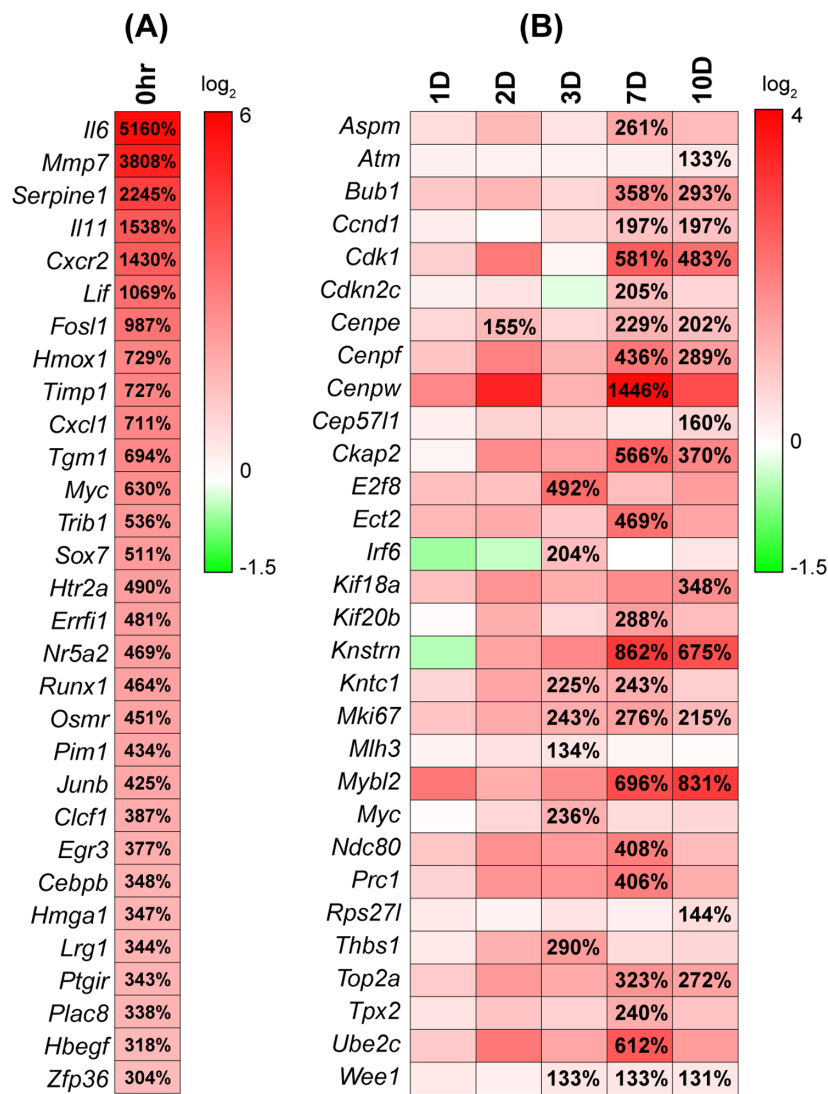
FIGURE 4. Cell proliferation related gene expression following PT-CEI. Genes in (**A**) likely represent signaling that occurs immediately following PT-CEI, while genes in (**B**) likely represent the evidence of ONH proliferation occurring 3 to 10 days following PT-CEI. Significant genes are only those *boxes* containing the extent of expression (in percentages relative to naïve ONH values). The most active cellular proliferation time points following PT-CEI were 3 to 10 days.

upregulated in the Chronic/Array study. Looking at specific genes of interest, we found that *Il6* and *Socs3* were significantly upregulated in the Chronic/Array study (*Il6* = 1553% and *Socs3* = 372%) and were only significantly upregulated at 0 hours in the PT-CEI/Seq study (*Il6* = 5160% and *Socs3* = 838%). Additionally, 6 of the 40 significantly upregulated *Immune Response*–related genes at 10 days in PT-CEI/Seq study were significantly upregulated in the Chronic/Array study. Looking at specific genes of interest, we found that *Anxa1* (149%) and *Fcerg1* (151%) were significantly upregulated in the Chronic/Array study and were only significantly upregulated at 10 days in the PT-CEI/Seq study.

Next, we assessed genes in common between the PT-CEI/Seq study and the FCG/Seq study.[11] Out of the 384 significant genes identified in the FCG/Seq study, we found that 36% of these were also significant at least at one time point following PT-CEI. Figure 7B shows that the number of significant genes in both studies was highest at the 0 hours time point of the PT-CEI study (61 genes) and decreased at

3 days (16 genes) and 7 days (14 genes), with a slight increase at 10 days (23 genes). Of these genes, most were regulated in the same direction in both studies (Fig.7B). Twelve of the 150 significantly upregulated *Defense Response* genes at 0 hours in the PT-CEI/Seq study were also significantly upregulated in the FCG/Seq study. Two of these genes, *Soc3* (367%) and *Cd44* (323%), were upregulated in all three studies. However, only 2 of the 40 significantly upregulated *Immune Response*–related genes at 10 days in the PT-CEI/Seq study were also significantly upregulated in the FCG/Seq study (*Rt1-Da* and *Lcp2*).

Cell cycle/cellular proliferation processes were the most common Gene Ontology clusters among all three studies (Figs. 8A, 8B). We found that several cell cycle genes previously identified in Figure 4B were also significantly regulated in the Chronic/Array or FCG/Seq studies (Fig. 8C). For example, *Cdk1* (1425%) was significantly upregulated in the Chronic/Array study and at 7 days (323%) and 10 days (272%) following PT-CEI (Fig. 8C). This further indicates that
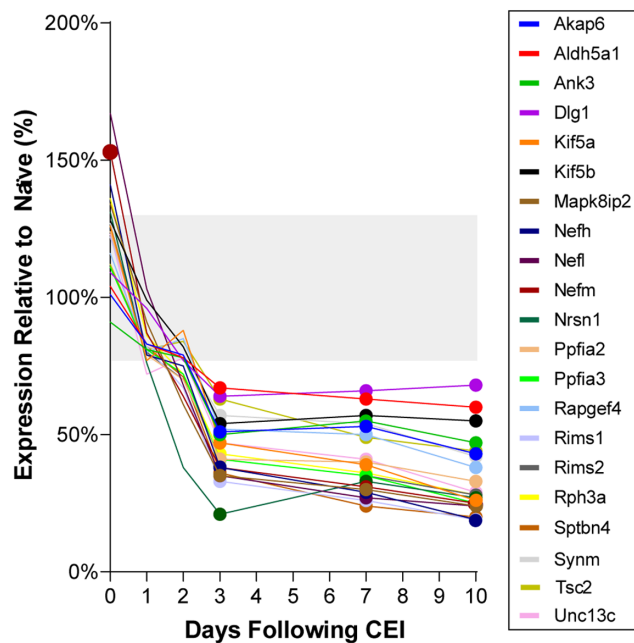
Investigative Ophthalmology & Visual Science

FIGURE 5. Axonally related mRNA expression in the ONH is dramatically depressed from 3 through 10 days following PT-CEI. Twenty-one genes were found to be related to the axon, axonal transport, the synapse, or synaptic transmission. Mean expression levels of these 21 genes decreased to near-minimal levels by 3 days with no evidence of recovery through 10 days. Only data points outside the *gray box* and identified by the *heavy dots* are significant (FDR ≤10%).

proliferation is a key cellular event that occurs in the ONH following exposure to elevated IOP.

Axonal/neuronal-related Gene Ontology clusters were significantly downregulated in both PT-CEI/Seq and Chronic/Array studies (Fig. 8A). For example, three axonal-related genes, *Gap43* (65%), *Mapt* (49%), and *Nefl* (22%), were significantly downregulated in the Chronic/Array study. In the PT-CEI/Seq study, *Gap43* was significantly downregulated at 3 days (34%) and 10 days (40%) following PT-CEI, while *Mapt* was significantly downregulated 3 days (48%) following PT-CEI. As shown in Figure 5, *Nefl* was persistently downregulated 3 days (35%), 7 days (27%), and 10 days (24%) following PT-CEI. These findings indicate that, at a few days after exposure to elevated IOP, downregulation in axonal-related mRNA expression can be detected. On the other hand, downregulated genes in common between the FCG/Seq and PT-CEI/Seq study did not cluster (Fig. 8B).

Astrocytes Likely Largely Responsible for RNA-Seq Cellular Responses Following PT-CEI

Astrocyte (Sox2$^+$ nuclei), oligodendroglia (Olig2$^+$ nuclei), and microglia/macrophages (Iba1$^+$ cells) were quantified in control and PT-CEI–exposed ONH (Fig. 9). In control ONH, there were significantly higher Sox2$^+$ nuclear densities (4812 ± 1869 nuclei/mm^2) than either Olig2 (484 ± 291 nuclei/mm^2; $P < 0.0001$) or Iba1 (414 ± 125 nuclei/mm^2; $P < 0.0001$). Sox2$^+$ nuclear densities significantly increased 3 days following PT-CEI (6735 ± 2238 nuclei/mm^2; $P = 0.03$). Olig2$^+$ nuclear densities did not change after PT-CEI. Iba1$^+$ nuclear densities significantly increased 3 days (740 ± 408 nuclei/mm^2; $P = 0.01$) and 7 days (973 ± 209 nuclei/mm^2;

$P < 0.0001$) following PT-CEI. These findings indicate that our RNA-seq results are likely largely an astrocytic response following PT-CEI, with some microglia/macrophage input.

DISCUSSION

Glaucoma pathogenesis is multifaceted, and evidence points to the ONH as the initial site of injury following elevated IOP.[4,7] The only treatable risk factor thus far is to lower IOP. Understanding the significance of ONH cellular responses to elevated IOP may yield new routes for therapeutic interventions that may be used in conjunction with current, IOP-lowering treatments. Several studies using models of chronic IOP elevation have revealed a large number of ONH cellular responses.[9,11,45] However, the relationship of these responses to IOP elevation and axonal injury is complicated by ongoing and fluctuating IOP. Thus, the difficulty of controlling IOP exposure elevation and duration consistently across animals in these models represents a limiting factor in our ability to determine mechanisms of axonal injury in experimental glaucoma.

In the current study, we utilized a model where a defined IOP level for a specific duration results in evidence of mild, focal optic nerve injury as early as 7 days after the exposure. Thus, it is possible to investigate the sequence of ONH cellular responses at specific time points following a single pressure stimulus, and their significance can be considered in the context of their temporal relationship to the IOP stimulus and to each other. Responses occurring during or shortly after IOP exposure would be more likely associated with axonal injury, while those that are delayed may represent a response to injury, as well as "downstream" pathways initiated by early events.

The PT-CEI model was specifically designed to maximize the stress–strain response of the ONH to IOP. IOP is increased to 60 mm Hg and then, every hour, lowered to 20 mm Hg (the normal mean awake rat IOP) for 5 minutes over a duration of 8 hours. It is important to note that in vivo measurements using optical coherence tomography angiography, as well as visible light OCT, have shown that retinal and ONH perfusion are maintained at this pressure.[24,41,42,46] We specifically showed that an IOP ≥70 mm Hg is needed to significantly decrease retinal blood flow. Interestingly, Bui and colleagues[47] showed that electroretinogram parameters recovered when IOP was elevated to 60 mm Hg or less for 105 minutes but not when IOP was ≥70 mm Hg. These findings indicate that retinal blood flow is maintained when IOP is ≤60 mm Hg. We also provide blood pressure measurements acquired during the PT-CEI experiment to show that an IOP of 60 mm Hg is considerably lower than diastolic blood pressure, indicating perfusion is maintained throughout the PT-CEI experiment (Supplementary Fig. S3). Additionally, in our original CEI study, we describe how the electroretinogram A and B waves did not significantly change after CEI.[20] Together with the lack of evidence in our RNA-seq data of hypoxia-related expression changes immediately following PT-CEI, these findings support that blood flow was not compromised during PT-CEI, and our results represent the direct and indirect responses of ONH tissues to increased IOP. Another important outcome of the present study is that there were negligible ONH mRNA expression changes after the normotensive CEI (IOP of 20 mm Hg). This supports the conclusion that mRNA expression changes after PT-CEI (IOP of 60 mm Hg) are due to elevated IOP and not to general anesthesia or the cannulation procedure.
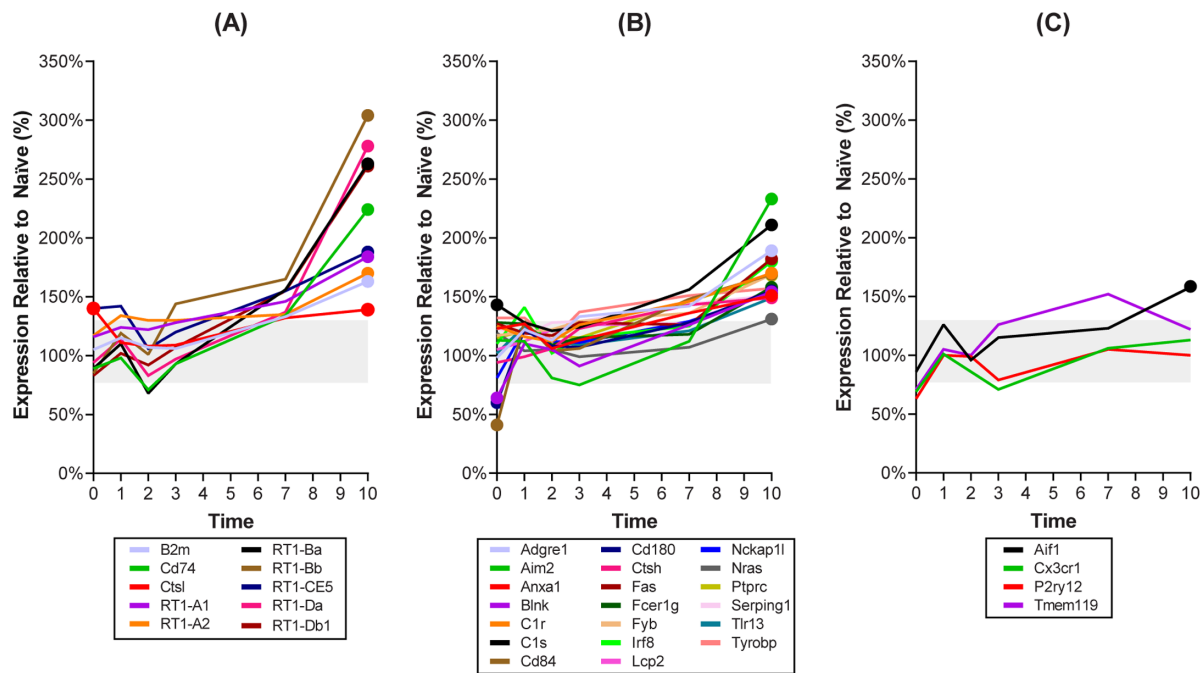
FIGURE 6. Immune-related mRNA expression slowly increased in regulation, reaching significance 10 days following PT-CEI, indicating development of a delayed *Immune Response*. (**A**) Ten genes were identified as being part of the "Antigen Processing and Presentation" Kyoto Encyclopedia of Genes and Genomes pathway, with only *Ctsl* being upregulated immediately (0 hours) and at 10 days after PT-CEI. (**B**) An additional 20 slightly upregulated genes were categorized as being immune-related genes with literature supporting their involvement with microglia/macrophages. Three of these genes were initially downregulated at 0 hours (*Blnk*, *Cd84*, *CD180*), while one was upregulated at 0 hours (*C1s*). (**C**) The common microglia/macrophage marker, *Aif1*, became significantly upregulated at 10 days, while *Cx3cr1*, *P2ry12*, and *Tmem119* were not significantly affected. Only data points outside the *gray box* and identified by *heavy dots* are significant (FDR ≤10%).

Comparison of PT-CEI With Chronic Models of Ocular Hypertension

Our comparison of ONH gene expression responses following PT-CEI to two models of chronically elevated IOP revealed several important similarities. We found that several genes in the Chronic/Array and PT-CEI/Seq studies were regulated in the same direction. For example, several *Defense Response*–related genes were upregulated in both studies (*Il6*, *Socs3*, *Lif*, *Anxa1*, and *Fcer1g*). But we were able to show that some of these were upregulated immediately following PT-CEI (*Il6*, *Socs3*, and *Lif*), while others became significantly upregulated (*Anxa1* and *Fcer1g*) 10 days following PT-CEI. The early upregulation of these Il6-type cytokines (*Il6*, *Socs3*, and *Lif*) further supports our previous findings that the Jak-Stat Signaling pathway is an early player in glaucomatous neurodegeneration.[9]

We also found that the most common Gene Ontology cluster among all three studies was cellular proliferation (Fig. 8C). However, there are likely differences in the cell types that are proliferating between studies. We previously reported that, following 5 weeks of chronically elevated IOP, astrocytes make up the majority of proliferating cells in ONHs, followed by microglia/macrophages, and reported no indication of oligodendroglia proliferation.[39] We also reported that astrocytes make up 78% of anterior ONH cells, similar to the ONH region analyzed in this RNA-seq study.[39] For additional comparison purposes, we found that Sox2 densities were significantly higher than either Olig2 or Iba1 densities in the first 400 µm posterior to Bruch's membrane

opening (Fig. 9). This region is comparable to the region analyzed in this current analysis, supporting the idea that astrocytes are largely driving the PT-CEI/Seq findings. Additionally, Olig2 nuclear densities did not change following PT-CEI. We previously reported that 22% of Sox2 nuclei colabeled with Olig2, further indicating minimal contribution of oligodendroglia to these responses.[39] There was a significant increase in microglia/macrophages 3 to 7 days following PT-CEI, likely indicating they contribute to delayed response following PT-CEI. Therefore, it is likely that the majority of proliferating cells after PT-CEI are astrocytes with some microglia/macrophage. In the FCG/Seq study, the majority of proliferating cells were microglia/macrophages (Iba1+ cells) in the prelamina and lamina cribrosa regions, as well as proliferating oligodendrocyte precursor cells in the retrolaminar region. We are in the process of quantifying cell proliferation following PT-CEI to determine if glial-type proliferation varies over days following exposure to elevated IOP.

In the PT-CEI/Seq study, we were able to show that axonal/neuronal genes are downregulated within days of exposure to elevated IOP and remain downregulated at least out to 10 days following a single exposure to elevated IOP. In the Chronic/Array study, several of these axonal/neuronal related genes were downregulated out to 5 weeks after exposure to chronically elevated IOP. These findings raise the possibility that persistent downregulation of these neuronal/axonal genes might render remaining axons more vulnerable to future IOP elevations. They also highlight the usefulness of identifying time-dependent ONH cellular
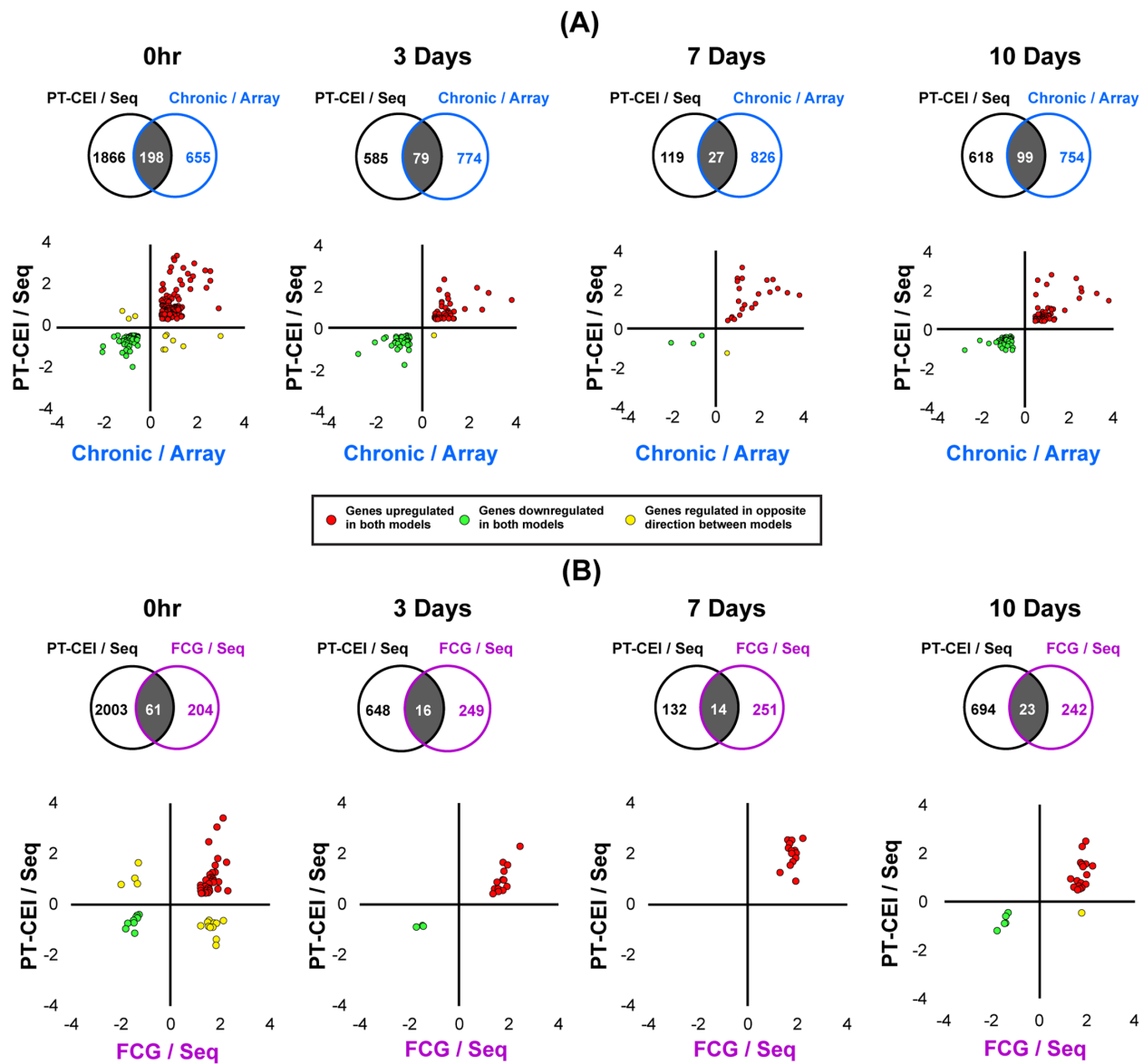
FIGURE 7. Comparison of elevated IOP-induced ONH gene expression responses in three experimental models. (**A**) The maximum number of genes in common between the PT-CEI/Seq study and the Chronic/Array study[9] occurred at 0 hours (198 genes in common) and 10 days (99 genes in common) following PT-CEI. Over 95% of these genes were regulated in the same direction (x–y scatterplots). (**B**) The maximum number of genes in common between the PT-CEI/Seq study and the FCG/Seq study[11] also occurred at 0 hours (61 genes in common) and 10 days (23 genes in common) following PT-CEI, and the majority of these genes were also regulated in the same direction (x–y scatterplots). For both **A** and **B**, *red points* in scatterplots indicate genes that are upregulated in both models, *green points* indicate genes that are downregulated in both models, and *yellow points* indicate genes that are regulated in the opposite direction between models. Notice how the majority of the points are either *red* or *green*, indicating that expression change direction agreed well between models.

responses to a single-pressure exposure that could shed light on their potential role be in eyes with chronic IOP elevation.

Early ONH Responses Following PT-CEI

The earliest events following PT-CEI were an upregulation in *Il6* and several other *Il6*-type cytokines that initiate signaling via the Jak-Stat pathway. This pathway initiates several processes, including cellular proliferation, and has been shown to regulate glial cell proliferation.[9,39,44,48–50] We identified the Gene Ontology clusters "Regulation of Cell Proliferation" as being significantly upregulated immediately following PT-CEI. This might indicate that proliferation signals are

some of the earliest events to occur following an elevated IOP event. The highly active 0 hours time point following PT-CEI was surprisingly followed by a quiet period of regulation lasting 1 to 2 days. This raises an interesting possibility of intervening with, for example, the Jak-Stat pathway, to tease apart its role with downstream pathways. Sun and colleagues[44] specifically targeted inhibition of STAT3, a member of the Jak-Stat pathway signaling family, and found astrocyte reactivity was attenuated but with a concomitant higher ganglion cell loss. This could indicate that STAT3 and/or the Jak-Stat pathway plays a protective role.

Other early cellular events immediately following PT-CEI was an upregulation of 150 *Defense Response*–related
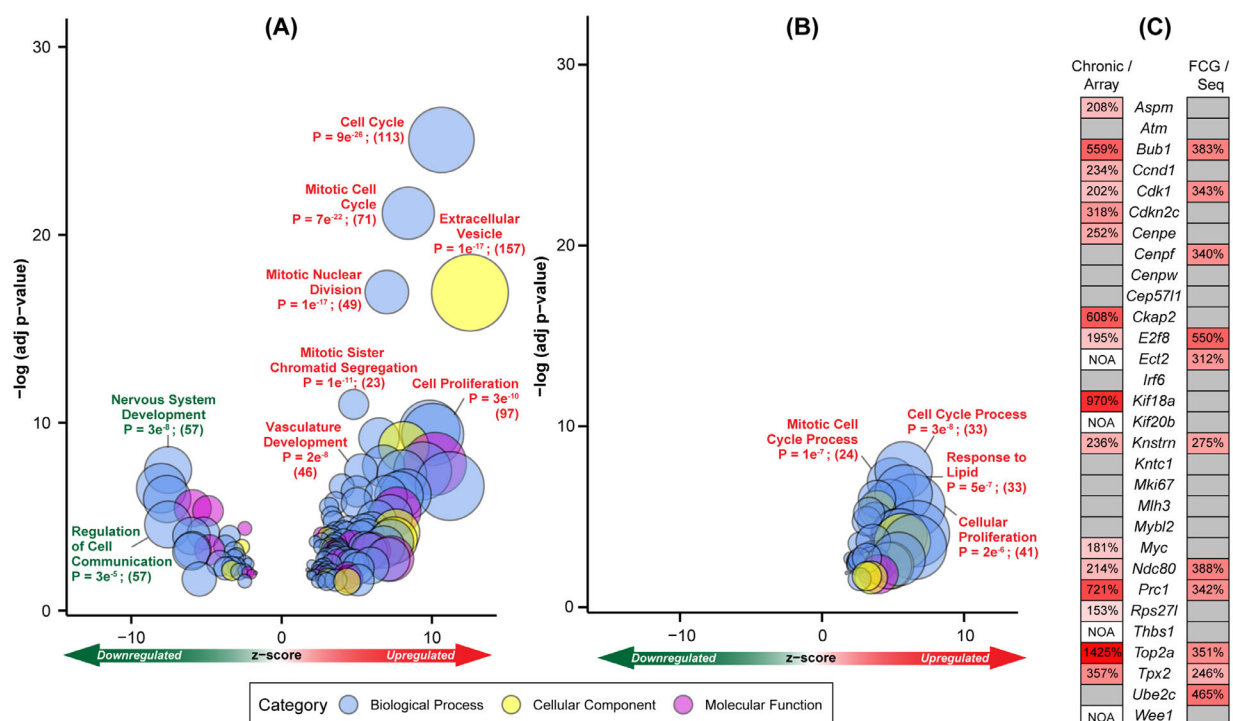
FIGURE 8. Functional analysis comparisons between two elevated IOP models. (**A**) GOPlots of significantly regulated Gene Ontology clusters from DAVID analysis (clusters with EASE score ≥1.3) from the Chronic/Array study. Downregulated genes were most frequently related to compromised neuronal/axonal-type terms while upregulated genes were mostly related to *Cell Cycle* Gene Ontology terms. (**B**) GOPlots of significantly regulated Gene Ontology clusters from DAVID analyses from the FCG/Seq study. There were no downregulated clusters and upregulated Gene Ontology clusters were most frequently related to *Cell Cycle Processes*. (**C**) Heatmap, with expression relative to naïve values indicated inside each *box*, of genes previously identified as being cell cycle related in our PT-CEI/Seq study. *Gray boxes* indicate nonsignificant genes. Genes not on array are indicated with NOA.

genes. The *Defense Response* cluster becomes nonsignificant 1 to 7 days following PT-CEI and reappears as an *Immune Response* cluster at 10 days. Importantly, mean expression of the top 10 *Defense Response*–related genes (Fig. 3A) was much higher (1791%) than the top 10 *Immune Response* genes (348%). This highlights that the early (0 hours) *Defense Response* is more robust than the delayed (10-day) *Immune Response*. Some *Defense Response* genes of interest include *Serpine1* (2245%), *Cxcr2* (1430%), *Sele* (1096%), and *Lcn2* (662%). *Serpine1* may modulate blood–brain barrier function, possibly tightening the endothelial barrier.[51,52] *Cxcr2* has been described in activated microglia in multiple sclerosis, Alzheimer's disease, and stroke.[53] It may also modulate optic nerve repair by regulating inflammatory cell infiltration and microglia activation.[54] *Sele* is a surface protein that is in endothelial cells and may mediate transient neutrophil adhesion.[55,56] *Lcn2* is associated with many functions, including immune response, cell proliferation, cell apoptosis, and iron delivery. We and others have shown that *Lcn2* is upregulated in the glaucomatous retina[57,58] and ONH.[9] While studies have shown that astrocytes express *Lcn2*,[59,60] others suggest that T cells express *Lcn2* in the microbead model and optic nerve crush (Vincent NH et al., *IOVS* 2018;59:ARVO E-Abstract 3745). The robust upregulation of these *Defense Response*–related genes indicates that they are likely to play an important and early role in glaucomatous neurodegeneration. These could either be protective or injurious, and a model that carefully controls the pressure stimulus could be an important tool in helping to sort this out.

ONH Axonal mRNA Expression Is Disproportionally Reduced Relative to Nerve Injury

Twenty-one axonal-related genes remained downregulated 3, 7, and 10 days following PT-CEI (Fig. 5). Some genes of interest include *Akap6*, *Kif5a*, and neurofilaments (*Nefh*, *Nefl*, and *Nefm*). Wang and colleagues[61] reported that *Akap6* is required for axon survival and growth of cultured primary RGCs. *Kif5a* plays a role in mitochondrial transport and is a principal anterograde motor for neurofilaments.[62] Previous work showed that mitochondrial density increases in the glaucomatous ONH.[4,63–65] Mitochondria play a crucial role in maintaining constant energy supply and are key regulators of several neuronal processes.[66] These include metabolic balance, production of reactive oxygen species, and apoptotic signaling. Neurofilaments play a key role in axon caliber and their signal conduction and are important regulators of mitochondrial morphology, dynamics, and motility.[67–69] All three neurofilaments (*Nefl*, *Nefm*, and *Nefh*) were significantly downregulated in the current study. The sustained downregulation of neurofilaments following PT-CEI is likely contributing toward modifying ONH mitochondrial transport and might subsequently impact axonal injury. The sustained decrease in these axonally associated mRNA was disproportionally greater than the amount of axon degeneration identified in histologic sections. This could result from impaired retinal ganglion cell function or sustained impairment in axonal transport. Better understanding of these mechanisms and why they persist well after
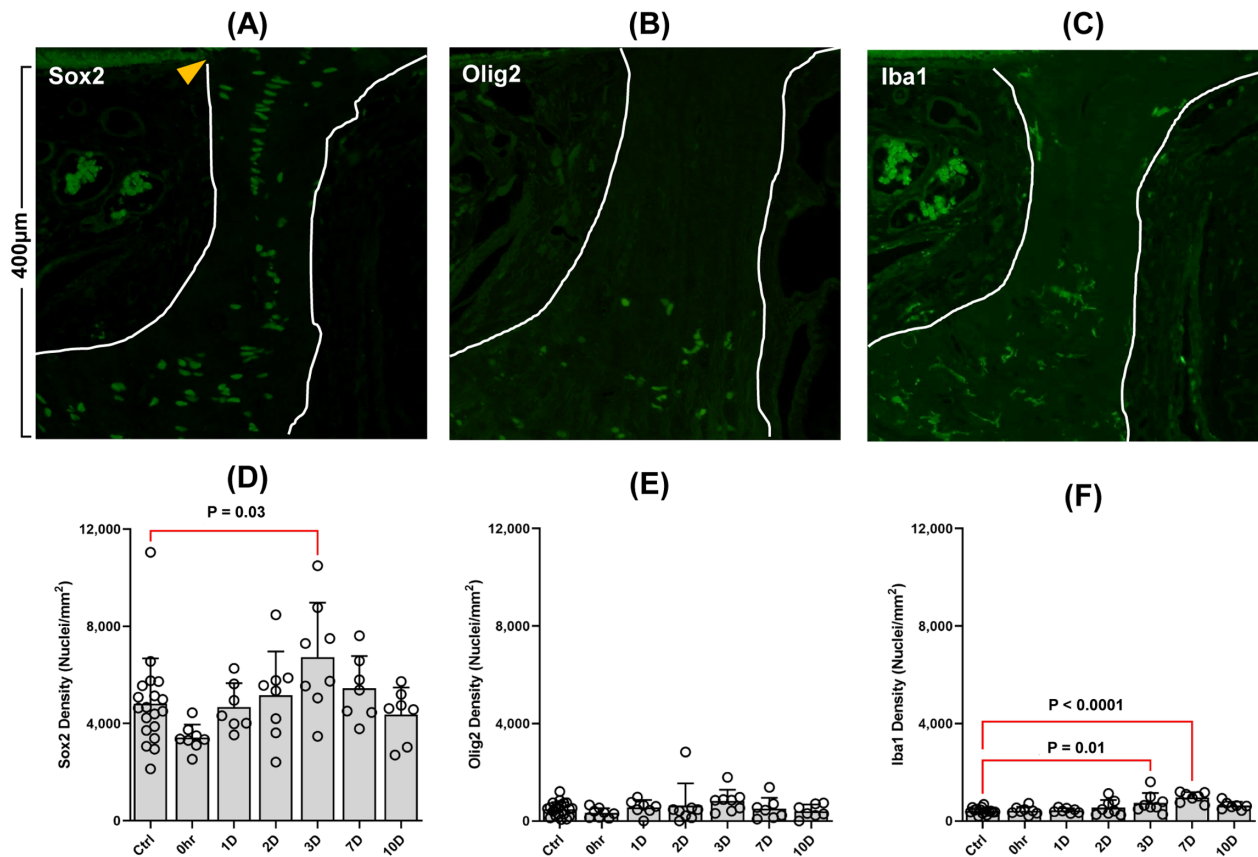
FIGURE 9. Immunolabeling of ONH glia following PT-CEI. (**A**) ONH astrocytes were immunolabeled with Sox2 (**A**), oligodendroglia with Olig2 (**B**), and microglia and macrophages with Iba1 (**C**) in control eyes ($n = 20$ eyes) and 0 hours to 10 days following PT-CEI ($n = 7$–8 eyes per experimental time point). Mean ± SD of (**D**) Sox2, (**E**) Olig2, and (**F**) Iba1 nuclear densities quantified in the first 400 µm posterior to Bruch's membrane opening (*orange arrowhead* in **A**). *White lines* in **A–C** delineate the boundaries of the ONH.

normalization of IOP will provide important insights for patients who continue to experience vision loss despite IOP control.

The current study highlights how a single elevated IOP exposure hinders axonal mRNA and raises the question of how much more susceptible these axons might be when they encounter another IOP elevation event or when they are under prolonged/chronically elevated IOP. Patients with glaucoma often exhibit fluctuation of IOP.[70,71] Yet, little is known of how prior injury or IOP fluctuations contribute to axonal injury. Our results indicate that further work with this paradigm has the potential to provide important clues to these intriguing questions.

Delayed Immune Responses Following PT-CEI

The delayed *Immune Response* observed 10 days following PT-CEI may reflect microglia, astrocytes, or endothelial cell function. Microglia provide neurotrophic support, promote tissue renewal through their phagocytic function, and are actively interacting and surveying surrounding neurons, blood–brain barrier cells, and other glia to detect changes in their homeostatic environment.[72,73] Microglia and astrocytes are thought to induce an immune response through expression of major histocompatibility complex (MHC) genes.[74,75] In the current study, we found 10 genes related to antigen-presenting processes that were significantly upregulated 10 days following PT-CEI, including several MHC genes

([Fig. 6](#)A). At the protein level, previous work has shown that optic nerve microglial expression of MHC class II (*Rt1b*) was associated with more severe axonal degeneration in a laser model of experimental glaucoma.[76] Put together, the delayed appearance of these *Immune Response* genes in our study suggests that they may be more part of a reactive process to axonal injury, rather than part of the initial injury process. However, as we are looking at responses to a single episode of pressure elevation, we cannot rule out the potential that delayed immune-related events may have important effects on the response and axonal susceptibility to subsequent pressure elevations and IOP fluctuation, as may be seen in chronic models and human glaucoma. Additional analysis of the response of cell types in association with specific gene changes using this model will be required to understand better the significance of these findings.

Other Genes of Potential Interest

Not surprisingly, ONH *GFAP* mRNA levels did not change after PT-CEI. While *GFAP* expression increases in the retina,[77–79] this is not the case in the ONH with mild axonal injury following IOP elevation. For example, in the hypertonic saline model, we reported that ONH GFAP labeling actually decreased 1 to 2 weeks after IOP was chronically elevated, and labeling only increased with glial scar formation.[80] In our other two studies, we found that *GFAP* mRNA levels did not change in nerves with mild injury

following 5 weeks of chronically elevated IOP.[7,9] The level of injury in these animals was comparable to the level of optic nerve injury observed in our current study. Similar findings are reported in the ONH in two other animal models (the feline congenital glaucoma model and the DBA2J mouse model). Oikawa and colleagues[11] found no significant change in ONH GFAP immunolabeling intensity and no mRNA level changes in astrocyte markers (*GFAP*, *VIM*, and *AQP4*). Howell and colleagues[45] found no significant change in GFAP mRNA in ONH with less than 30% axon degeneration. While GFAP labeling and expression have been used to determine astrocytic response to elevated IOP, these alone are not sufficient markers to broadly categories astrocytic responses. It is more likely that multiple parameters (e.g., a set of genes, shape quantification, immunolabeling by several markers, astrocytic maturity) will be needed to fully understand astrocytic responses to the injurious process following elevated IOP.

Other genes of interest previously identified from the literature to likely play a role in glaucomatous damage include tumor necrosis factor alpha (*Tnf*), nitric oxide synthase 2 (*Nos2*), and endothelin 1 and endothelin 2 (*Edn1* and *Edn2*). Increased levels of *Tnf* have been associated with retinal ganglion cell death, but this gene was not detectable at any time point in our current PT-CEI study.[81–83] Additionally, we did not find evidence of *Nos2* changing following PT-CEI, in agreement with our previous findings.[84] We did find that *Edn1* was significantly upregulated (216%), but only immediately after PT-CEI. Elevated levels of *Edn1* have been suggested to negatively impact ONH blood flow and retinal ganglion cell viability.[85,86] *Edn2* was significantly upregulated in the DBA/2J mouse ONH and retina, likely contributing to vasoconstriction.[45] However, *Edn2* was not detected in this current study.

The appearance of these immune-related responses following PT-CEI also prompted us to investigate the involvement of the complement pathway (Supplementary Table S3). This pathway has been shown to be activated in the DBA/2J mouse model, with *C1qa* shown to be protective, while *C3* deficiency was correlated with greater damage.[10,45,87] We found that neither *C1qa* nor *C3* were significantly regulated at any time point following PT-CEI. However, other complement genes were mildly upregulated at 0 hours (*C1qb*, *C1qc*, *C1qbp*, and *C1s*), and some were also upregulated at 10 days (*C1r* and *C1s*). The mild upregulation of *C1qb* (159%), *C1qc* (150%), and *C1s* (143%) immediately following PT-CEI could indicate an early activation of the classical component pathway. However, their levels were quite low in comparison to other genes that were significantly upregulated at 0 hours, and they were not among the top 100 significantly upregulated genes immediately following PT-CEI. Thus, our findings suggest that the complement pathway in the ONH plays a limited role in responding to a single exposure to elevated IOP, although more extensive regulation might occur with prolonged or repeated exposures to elevated IOP.

In conclusion, this study highlights that the ONH microenvironment is altered for days after a single, short-term elevated IOP exposure and that this paradigm can be used to successfully model sequential events of chronic glaucoma. Knowing the time-dependent events is critical to identify possible routes for therapeutic intervention. For example, we can begin to test whether inhibiting or enhancing specific pathways at specific time points following PT-CEI are beneficial or detrimental.

Disclosure: **D.C. Lozano**, None; **H. Jayaram**, None; **W.O. Cepurna**, None; **S. Tehrani**, None; **L. Gao**, None; **S.S. Fei**, None; **D. Choi**, None; **E.C. Johnson**, None; **J.C. Morrison**, None

References

1. Collaborative Normal-Tension Glaucoma Study Group. The effectiveness of intraocular pressure reduction in the treatment of normal-tension glaucoma. *Am J Ophthalmol*. 1998;126:498–505.
2. Anderson DR. The management of elevated intraocular pressure with normal optic discs and visual fields. I. Therapeutic approach based on high risk factors. *Surv Ophthalmol*. 1977;21:479–489.
3. Nickells RW, Schlamp CL, Li Y, et al. Surgical lowering of elevated intraocular pressure in monkeys prevents progression of glaucomatous disease. *Exp Eye Res*. 2007;84:729–736.
4. Quigley HA, Addicks EM, Green WR, Maumenee AE. Optic nerve damage in human glaucoma. II. The site of injury and susceptibility to damage. *Arch Ophthalmol*. 1981;99:635–649.
5. Schlamp CL, Li Y, Dietz JA, Janssen KT, Nickells RW. Progressive ganglion cell loss and optic nerve degeneration in DBA/2J mice is variable and asymmetric. *BMC Neurosci*. 2006;7:66.
6. Howell GR, Libby RT, Jakobs TC, et al. Axons of retinal ganglion cells are insulted in the optic nerve early in DBA/2J glaucoma. *J Cell Biol*. 2007;179:1523–1537.
7. Johnson EC, Jia L, Cepurna WO, Doser TA, Morrison JC. Global changes in optic nerve head gene expression after exposure to elevated intraocular pressure in a rat glaucoma model. *Invest Ophthalmol Vis Sci*. 2007;48:3161–3177.
8. Kompass KS, Agapova OA, Li W, Kaufman PL, Rasmussen CA, Hernandez MR. Bioinformatic and statistical analysis of the optic nerve head in a primate model of ocular hypertension. *BMC Neurosci*. 2008;9:93.
9. Johnson EC, Doser TA, Cepurna WO, et al. Cell proliferation and interleukin-6-type cytokine signaling are implicated by gene expression responses in early optic nerve head injury in rat glaucoma. *Invest Ophthalmol Vis Sci*. 2011;52:504–518.
10. Harder JM, Braine CE, Williams PA, et al. Early immune responses are independent of RGC dysfunction in glaucoma with complement component C3 being protective. *Proc Natl Acad Sci USA*. 2017;114:E3839–E3848.
11. Oikawa K, Ver Hoeve JN, Teixeira LBC, et al. Sub-region-specific optic nerve head glial activation in glaucoma. *Mol Neurobiol*. 2020;57:2620–2638.

12. Williams PA, Marsh-Armstrong N, Howell GR, IIoA Lasker; Glaucomatous Neurodegeneration Participants. Neuroinflammation in glaucoma: a new opportunity. *Exp Eye Res*. 2017;157:20–27.

13. Rolle T, Ponzetto A, Malinverni L. The role of neuroinflammation in glaucoma: an update on molecular mechanisms and new therapeutic options. *Front Neurol*. 2020;11:612422.

14. Quaranta L, Bruttini C, Micheletti E, et al. Glaucoma and neuroinflammation: an overview. *Surv Ophthalmol*. 2021;66:693–713.

15. Morrison JC, Cepurna WO, Johnson EC. Modeling glaucomatous optic nerve damage. *Int Ophthalmol Clin*. 1999;39:29–41.

16. Pang IH, Clark AF. Rodent models for glaucoma retinopathy and optic neuropathy. *J Glaucoma*. 2007;16:483–505.

17. Rasmussen CA, Kaufman PL. Primate glaucoma models. *J Glaucoma*. 2005;14:311–314.

18. Weinreb RN, Lindsey JD. The importance of models in glaucoma research. *J Glaucoma*. 2005;14:302–304.

19. McKinnon SJ, Schlamp CL, Nickells RW. Mouse models of retinal ganglion cell death and glaucoma. *Exp Eye Res*. 2009;88:816–824.

20. Morrison JC, Cepurna WO, Tehrani S, et al. A period of controlled elevation of IOP (CEI) produces the specific gene expression responses and focal injury pattern of experimental rat glaucoma. *Invest Ophthalmol Vis Sci*. 2016;57:6700–6711.

21. Morrison JC, Moore CG, Deppmeier LM, Gold BG, Meshul CK, Johnson EC. A rat model of chronic pressure-induced optic nerve damage. *Exp Eye Res*. 1997;64:85–96.

22. ARVO. Statement for the Use of Animals in Ophthalmic and Vision Research. 2016, https://www.arvo.org/About/policies/arvo-statement-for-the-use-of-animals-in-ophthalmic-and-vision-research/.

23. Burgoyne CF, Downs JC, Bellezza AJ, Suh JK, Hart RT. The optic nerve head as a biomechanical structure: a new paradigm for understanding the role of IOP-related stress and strain in the pathophysiology of glaucomatous optic nerve head damage. *Prog Retin Eye Res*. 2005;24:39–73.

24. Pi S, Hormel TT, Wei X, et al. Monitoring retinal responses to acute intraocular pressure elevation in rats with visible light optical coherence tomography. *Neurophotonics*. 2019;6:041104.

25. Jayaram H, Lozano DC, Johnson EC, Morrison JC. Investigation of MicroRNA expression in experimental glaucoma. *Methods Mol Biol*. 2018;1695:287–297.

26. Bolger AM, Lohse M, Usadel B. Trimmomatic: a flexible trimmer for Illumina sequence data. *Bioinformatics*. 2014;30:2114–2120.

27. Dobin A, Davis CA, Schlesinger F, et al. STAR: ultrafast universal RNA-seq aligner. *Bioinformatics*. 2013;29:15–21.

28. DeLuca DS, Levin JZ, Sivachenko A, et al. RNA-SeQC: RNA-seq metrics for quality control and process optimization. *Bioinformatics*. 2012;28:1530–1532.

29. Chen Y, Lun AT, Smyth GK. From reads to genes to pathways: differential expression analysis of RNA-Seq experiments using Rsubread and the edgeR quasi-likelihood pipeline. *F1000Res*. 2016;5:1438.

30. Robinson MD, Oshlack A. A scaling normalization method for differential expression analysis of RNA-seq data. *Genome Biol*. 2010;11:R25.

31. Law CW, Chen Y, Shi W, Smyth GK. voom: precision weights unlock linear model analysis tools for RNA-seq read counts. *Genome Biol*. 2014;15:R29.

32. Benjamin Y, Hochberg Y. Controlling the false discovery rate: of practical and powerful approach two multiple testing. *J R Stat Soc B Methodol*. 1995;57:289–300.

33. Ritchie ME, Phipson B, Wu D, et al. limma powers differential expression analyses for RNA-sequencing and microarray studies. *Nucleic Acids Res*. 2015;43:e47.

34. da Huang W, Sherman BT, Lempicki RA. Systematic and integrative analysis of large gene lists using DAVID bioinformatics resources. *Nat Protoc*. 2009;4:44–57.

35. Huang da W, Sherman BT, Lempicki RA. Bioinformatics enrichment tools: paths toward the comprehensive functional analysis of large gene lists. *Nucleic Acids Res*. 2009;37:1–13.

36. Walter W, Sanchez-Cabo F, Ricote M. GOplot: an R package for visually combining expression data with functional analysis. *Bioinformatics*. 2015;31:2912–2914.

37. Jia L, Cepurna WO, Johnson EC, Morrison JC. Patterns of intraocular pressure elevation after aqueous humor outflow obstruction in rats. *Invest Ophthalmol Vis Sci*. 2000;41:1380–1385.

38. Cunningham F, Allen JE, Allen J, et al. Ensembl 2022. *Nucleic Acids Res*. 2022;50:D988–D995.

39. Lozano DC, Choe TE, Cepurna WO, Morrison JC, Johnson EC. Early optic nerve head glial proliferation and jak-stat pathway activation in chronic experimental glaucoma. *Invest Ophthalmol Vis Sci*. 2019;60:921–932.

40. Kuwabara K, Matsumoto M, Ikeda J, et al. Purification and characterization of a novel stress protein, the 150-kDa oxygen-regulated protein (ORP150), from cultured rat astrocytes and its expression in ischemic mouse brain. *J Biol Chem*. 1996;271:5025–5032.

41. Zhi Z, Cepurna WO, Johnson EC, Morrison JC, Wang RK. Impact of intraocular pressure on changes of blood flow in the retina, choroid, and optic nerve head in rats investigated by optical microangiography. *Biomed Opt Express*. 2012;3:2220–2233.

42. Zhi Z, Cepurna W, Johnson E, Jayaram H, Morrison J, Wang RK. Evaluation of the effect of elevated intraocular pressure and reduced ocular perfusion pressure on retinal capillary bed filling and total retinal blood flow in rats by OMAG/OCT. *Microvasc Res*. 2015;101:86–95.

43. Shaulian E, Karin M. AP-1 in cell proliferation and survival. *Oncogene*. 2001;20:2390–2400.

44. Sun D, Moore S, Jakobs TC. Optic nerve astrocyte reactivity protects function in experimental glaucoma and other nerve injuries. *J Exp Med*. 2017;214:1411–1430.

45. Howell GR, Macalinao DG, Sousa GL, et al. Molecular clustering identifies complement and endothelin induction as early events in a mouse model of glaucoma. *J Clin Invest*. 2011;121:1429–1444.

46. Zhi Z, Cepurna W, Johnson E, Shen T, Morrison J, Wang RK. Volumetric and quantitative imaging of retinal blood flow in rats with optical microangiography. *Biomed Opt Express*. 2011;2:579–591.

47. Bui BV, Batcha AH, Fletcher E, Wong VH, Fortune B. Relationship between the magnitude of intraocular pressure during an episode of acute elevation and retinal damage four weeks later in rats. *PLoS One*. 2013;8:e70513.

48. Nakanishi M, Niidome T, Matsuda S, Akaike A, Kihara T, Sugimoto H. Microglia-derived interleukin-6 and leukaemia inhibitory factor promote astrocytic differentiation of neural stem/progenitor cells. *Eur J Neurosci*. 2007;25:649–658.

49. Mi H, Haeberle H, Barres BA. Induction of astrocyte differentiation by endothelial cells. *J Neurosci*. 2001;21:1538–1547.

50. Bauer S. Cytokine control of adult neural stem cells. *Ann N Y Acad Sci*. 2009;1153:48–56.

51. Dohgu S, Takata F, Matsumoto J, et al. Autocrine and paracrine up-regulation of blood-brain barrier function by plasminogen activator inhibitor-1. *Microvasc Res*. 2011;81:103–107.

Investigative Ophthalmology & Visual Science

52. Hultman K, Bjorklund U, Hansson E, Jern C. Potentiating effect of endothelial cells on astrocytic plasminogen activator inhibitor type-1 gene expression in an in vitro model of the blood-brain barrier. *Neuroscience*. 2010;166:408–415.

53. Valles A, Grijpink-Ongering L, de Bree FM, Tuinstra T, Ronken E. Differential regulation of the CXCR2 chemokine network in rat brain trauma: implications for neuroimmune interactions and neuronal survival. *Neurobiol Dis*. 2006;22:312–322.

54. Liu YF, Liang JJ, Ng TK, et al. CXCL5/CXCR2 modulates inflammation-mediated neural repair after optic nerve injury. *Exp Neurol*. 2021;341:113711.

55. Carlos T, Kovach N, Schwartz B, et al. Human monocytes bind to two cytokine-induced adhesive ligands on cultured human endothelial cells: endothelial-leukocyte adhesion molecule-1 and vascular cell adhesion molecule-1. *Blood*. 1991;77:2266–2271.

56. Fries JW, Williams AJ, Atkins RC, Newman W, Lipscomb MF, Collins T. Expression of VCAM-1 and E-selectin in an in vivo model of endothelial activation. *Am J Pathol*. 1993;143:725–737.

57. Guo Y, Johnson EC, Cepurna WO, Dyck JA, Doser T, Morrison JC. Early gene expression changes in the retinal ganglion cell layer of a rat glaucoma model. *Invest Ophthalmol Vis Sci*. 2011;52:1460–1473.

58. Panagis L, Zhao X, Ge Y, Ren L, Mittag TW, Danias J. Gene expression changes in areas of focal loss of retinal ganglion cells in the retina of DBA/2J mice. *Invest Ophthalmol Vis Sci*. 2010;51:2024–2034.

59. Lee S, Park JY, Lee WH, et al. Lipocalin-2 is an autocrine mediator of reactive astrocytosis. *J Neurosci*. 2009;29:234–249.

60. Bi F, Huang C, Tong J, et al. Reactive astrocytes secrete lcn2 to promote neuron death. *Proc Natl Acad Sci USA*. 2013;110:4069–4074.

61. Wang Y, Cameron EG, Li J, et al. Muscle A-kinase anchoring protein-alpha is an injury-specific signaling scaffold required for neurotrophic- and cyclic adenosine monophosphate-mediated survival. *EBioMedicine*. 2015;2:1880–1887.

62. Uchida A, Alami NH, Brown A. Tight functional coupling of kinesin-1A and dynein motors in the bidirectional transport of neurofilaments. *Mol Biol Cell*. 2009;20:4997–5006.

63. Minckler DS, Bunt AH, Klock IB. Radioautographic and cytochemical ultrastructural studies of axoplasmic transport in the monkey optic nerve head. *Invest Ophthalmol Vis Sci*. 1978;17:33–50.

64. Coughlin L, Morrison RS, Horner PJ, Inman DM. Mitochondrial morphology differences and mitophagy deficit in murine glaucomatous optic nerve. *Invest Ophthalmol Vis Sci*. 2015;56:1437–1446.

65. Zhou DB, Castanos MV, Geyman L, et al. Mitochondrial dysfunction in primary open-angle glaucoma characterized by flavoprotein fluorescence at the optic nerve head. *Ophthalmol Glaucoma*. 2022;5:413–420.

66. Ito YA, Di Polo A. Mitochondrial dynamics, transport, and quality control: a bottleneck for retinal ganglion cell viability in optic neuropathies. *Mitochondrion*. 2017;36:186–192.

67. Gentil BJ, Minotti S, Beange M, Baloh RH, Julien JP, Durham HD. Normal role of the low-molecular-weight neurofilament protein in mitochondrial dynamics and disruption in Charcot-Marie-Tooth disease. *FASEB J*. 2012;26:1194–1203.

68. Didonna A, Opal P. The role of neurofilament aggregation in neurodegeneration: lessons from rare inherited neurological disorders. *Mol Neurodegener*. 2019;14:19.

69. Gafson AR, Barthelemy NR, Bomont P, et al. Neurofilaments: neurobiological foundations for biomarker applications. *Brain*. 2020;143:1975–1998.

70. Caprioli J, Coleman AL. Intraocular pressure fluctuation a risk factor for visual field progression at low intraocular pressures in the advanced glaucoma intervention study. *Ophthalmology*. 2008;115:1123–1129.e1123.

71. Kim JH, Caprioli J. Intraocular pressure fluctuation: is it important? *J Ophthalmic Vis Res*. 2018;13:170–174.

72. Wake H, Moorhouse AJ, Jinno S, Kohsaka S, Nabekura J. Resting microglia directly monitor the functional state of synapses in vivo and determine the fate of ischemic terminals. *J Neurosci*. 2009;29:3974–3980.

73. Ransohoff RM, Perry VH. Microglial physiology: unique stimuli, specialized responses. *Annu Rev Immunol*. 2009;27:119–145.

74. Perry VH. A revised view of the central nervous system microenvironment and major histocompatibility complex class II antigen presentation. *J Neuroimmunol*. 1998;90:113–121.

75. Sobue A, Ito N, Nagai T, et al. Astroglial major histocompatibility complex class I following immune activation leads to behavioral and neuropathological changes. *Glia*. 2018;66:1034–1052.

76. Chidlow G, Ebneter A, Wood JP, Casson RJ. Evidence supporting an association between expression of major histocompatibility complex II by microglia and optic nerve degeneration during experimental glaucoma. *J Glaucoma*. 2016;25:681–691.

77. Wang X, Tay SS, Ng YK. An immunohistochemical study of neuronal and glial cell reactions in retinae of rats with experimental glaucoma. *Exp Brain Res*. 2000;132:476–484.

78. Lam TT, Kwong JM, Tso MO. Early glial responses after acute elevated intraocular pressure in rats. *Invest Ophthalmol Vis Sci*. 2003;44:638–645.

79. Guo Y, Cepurna WO, Dyck JA, Doser TA, Johnson EC, Morrison JC. Retinal cell responses to elevated intraocular pressure: a gene array comparison between the whole retina and retinal ganglion cell layer. *Invest Ophthalmol Vis Sci*. 2010;51:3003–3018.

80. Johnson EC, Deppmeier LM, Wentzien SK, Hsu I, Morrison JC. Chronology of optic nerve head and retinal responses to elevated intraocular pressure. *Invest Ophthalmol Vis Sci*. 2000;41:431–442.

81. Yuan L, Neufeld AH. Tumor necrosis factor-alpha: a potentially neurodestructive cytokine produced by glia in the human glaucomatous optic nerve head. *Glia*. 2000;32:42–50.

82. Agarwal R, Agarwal P. Glaucomatous neurodegeneration: an eye on tumor necrosis factor-alpha. *Indian J Ophthalmol*. 2012;60:255–261.

83. Hu X, Xu MX, Zhou H, et al. Tumor necrosis factor-alpha aggravates gliosis and inflammation of activated retinal Muller cells. *Biochem Biophys Res Commun*. 2020;531:383–389.

84. Pang IH, Johnson EC, Jia L, et al. Evaluation of inducible nitric oxide synthase in glaucomatous optic neuropathy and pressure-induced optic nerve damage. *Invest Ophthalmol Vis Sci*. 2005;46:1313–1321.

85. Orgul S, Cioffi GA, Bacon DR, Van Buskirk EM. An endothelin-1-induced model of chronic optic nerve ischemia in rhesus monkeys. *J Glaucoma*. 1996;5:135–138.

86. Chauhan BC, LeVatte TL, Jollimore CA, et al. Model of endothelin-1-induced chronic optic neuropathy in rat. *Invest Ophthalmol Vis Sci*. 2004;45:144–152.

87. Williams PA, Tribble JR, Pepper KW, et al. Inhibition of the classical pathway of the complement cascade prevents early dendritic and synaptic degeneration in glaucoma. *Mol Neurodegener*. 2016;11:26.

Investigative Ophthalmology & Visual Science